Predicting Drought and Subsidence Risks in France

Charpentier Arthur[1], James Molly[2], and Ali Hani[3]

[1]UQAM, Université du Québec à Montréal (UQAM), Montréal (Québec), Canada
[2]EURo Institut d'Actuariat (EURIA), Université de Brest, France
[3]Willis Re, Paris, France

Correspondence: Arthur Charpentier (charpentier.arthur@uqam.ca)

Abstract. The economic consequences of drought episodes are increasingly important although they are often difficult to apprehend in part because of the complexity of the underlying mechanisms. In this article we will study one of the consequences of drought, namely the risk of subsidence (or more specifically clay shrinkage induced subsidence), for which insurance has been mandatory in France for several decades. Using data obtained from several insurers, representing about a quarter of the household insurance market over the past twenty years, we propose some statistical models to predict the frequency but also the intensity of these droughts for insurers. But even if we use more advanced models than standard regression-type models (here random forests to capture non linearity and cross effects), it is still difficult to predict the economic cost of subsidence claims even if all geophysical and climatic information is available.

1 Introduction

Climate change is a challenge for the insurance industry since risks are increasing in terms of frequency and intensity, as discussed in McCullough (2004), Mills (2007), Charpentier (2008) or Schwarze et al. (2011). In this article, we will see if it is possible to predict for a given year the costs associated with drought, and more specifically here, clay shrinkage induced subsidence in France.

1.1 Droughts, economic impacts, insurance coverage and climate change

In a seminal book published twenty years ago, Bradford (2000) started to address the problem of getting a better understanding of the connections between drought and climate change, already suggesting that the frequency and the intensity of such events could increase in the future. And in the more recent book, Iglesias et al. (2019) provided additional evidence about the influence of climate change on meteorological droughts in Europe. Ionita and Nagavciuc (2021) studied the temporal evolution of three drought indices over 120 years (the standardized precipitation index – SPI, the standardized precipitation evapo-transpiration index – SPEI, and the self-calibrated Palmer drought severity index – scPDSI). This updated study regarding the trends and changes in drought frequency in Europe concluded that most of the severe drought events occurred in the last two decades, corresponding to the time after the publication of Lloyd-Hughes and Saunders (2002) for example. Similarly, Spinoni et al. (2015) and Spinoni et al. (2017) (studying more specifically Europe, following their initial worldwide study in Spinoni et al. (2014)) observed that for both frequency and severity, the evolution towards drier conditions is more relevant in the last three

25   decades over Central Europe in spring, the Mediterranean area in summer, and Eastern Europe in autumn (using also multiple indices, over 60 years).

Regarding economic impacts, Hagenlocher et al. (2019) presents the outcomes of a systematic literature review, over the past twenty years, on people-centered drought vulnerability and risk conceptualization and assessments. Despite major advances over the past decades in terms of developing better methods and tools for characterizing individual components of risk, Hagen-

30   locher et al. (2019) mentioned persistent knowledge gaps which need to be confronted in order to advance the understanding of drought risk for people and policymakers, to move towards a more drought resilient society. Naumann et al. (2021) shows that (in Europe), drought damages, not related to subsidence or building damages but mainly agricultural losses, could strongly increase with global warming and cause a regional imbalance in future drought impacts. They provide some forecasts, under the assumption of absence of climate action (+4°C in 2100 and no adaptation), annual drought losses in the European Union

35   and United Kingdom combined are projected to rise to more than 65 billion € per year compared with 9 billion € per year currently, still still "two times larger when expressed to the relative size of the economy"(expressed as a fraction of the GDP). Note that this corresponds to the general feeling of the insurance industry: Bevere and Weigel (2021) suggests that current drought trends and corresponding economic risks will further aggravate under climate change.

But at the same time, Naumann et al. (2015) point out that related direct and indirect impacts are often difficult to quantify. A

40   key issue is that the lack of sufficient quantitative impact data makes it complicated to construct a robust relationship between the severity of drought events and related damages. Insurance coverage for drought has been intensively studied when related to agriculture. Iglesias et al. (2019) mention some drought insurance schemes with both indemnity based mechanisms and drought index based insurance, in Section 2.8. Vroege et al. (2019) provide an overview of index-based insurance in Europe and North America in the context of droughts, while Bucheli et al. (2021) focus on Germany. Note that Tsegai and Kaushik

45   (2019) address the importance of designing insurance products which do not only address drought impacts but also minimize land degradation. Besides this theoretical work, some countries provide actual covers for such risks. For example in Spain, it is possible to insure rain-fed crops against drought, as discussed in Entidad Estatal de Seguros Agrarios (ENESA) (2012), but in most countries drought coverage only concerns agricultural (crop) insurance, in the same way that frost is covered (see also Pérez-Blanco et al. (2017)).

50 ## 1.2   From drought to subsidence

In this article we will use data from several insurance companies in France regarding a very specific drought related peril, that is clay shrinkage induced subsidence, which causes damage to buildings. Without buildings to suffer from subsidence, there is no risk of damage. In turn, the risk of building damage is only part of the wider scope of economic impacts of this (drought-induced) subsidence (as describe in Kok and Costa (2021)). If clay shrinkage induced subsidence is now a

55   well known peril (or at least recognized as a major peril, see for instance Doornkamp (1993), or Brignall et al. (2002) which assessed the potential effects of climate change on clay shrinkage-induced land subsidence), insurance coverage for subsidence is still uncommon. Almost twenty years ago, as indicated in McCullough (2004), while perils related to earth movement were

traditionally excluded from most property policies, several states (in the United States of America) added mandated coverage for some subsidence related claims (with several limitations). And recently, Herrera-García et al. (2021) proved that subsidence

60 permanently reduces aquifer-system storage capacity, causes earth fissures, damages buildings and civil infrastructure, and increases flood susceptibility and risk. From an insurer's perspective, Wües et al. (2011) pointed out that as incidents of soil subsidence increase in frequency and severity with climate change, there is a need for systematic managing of the risks through a combination of loss prevention and risk transfer initiatives (such as insurance).

In France, subsidence is a phenomenon covered by all private property insurance covers, and that enters the scope of the

65 government backed French natural catastrophe regime provided by the *Caisse Centrale de Réassurance* (CCR). It is the second most important peril in terms of costs that the system covers (the first being floods, see Charpentier et al. (2021) for a recent discussion about flood events in France, in the context of climate change). Subsidence risk is defined (Ministère de la transition écologique et solidaire (MTES) (2016)) as the displacement of the ground surface due to shrinkage and swelling of clayey soils. It is due mainly to the presence of clay in the soil which swells in humid conditions and shrinks in dry ones, thus

70 creating instabilities in the terrain under constructions causing cracks to appear on the floor and walls which can jeopardise the solidity of the building. France, having a temperate climate, has saturated clayey soils, making subsidence predominant during droughts.

However, the past few years have seen this risk exacerbated by the extreme heat waves and lack of rainfall in France (see Caisse Centrale de Réassurance (CCR) (2019)) causing more and more subsidence claims, with little hope of this tendency

75 stopping given the current climate change context. Indeed, 37% of the total costs of natural catastrophes in France between 1982 and 2020 are caused by subsidence, 38% of which are concentrated over the period 2015-2019, which represents 15% of the total time that subsidence coverage has been in place (as discussed in Mission des Risques Naturels (MRN) (2021)). Furthermore, Soubeyroux et al. (2011) show that the frequency and intensity of heat waves and droughts will inevitably increase in the coming century in continental France and new areas that so far have been protected from drought will be at risk.

80 Additionally, AFFA [2015] predict that the cost of geotechnical droughts will nearly triple in 2040. More recently, the French Geological Survey (BRGM, *Bureau de Recherches Géologiques et Minières*) published a study, Gourdier and Plat (2018), describing extreme historical subsidence events as well as forecasts using various climate change scenarios. It found that the first third of the century will suffer from unusual droughts in both their intensity and spatial expansion: one in three summers between 2020 and 2050 and one in two summers between 2050 and 2080 are to be as extreme as the summer of 2003 in

85 continental France (the worst subsidence event ever registered by the CCR, see Corti et al. (2009) that focused on the 2003 heatwave in France). Looking at the most pessimistic scenario, a 2003 type event might occur half of the time between 2020 and 2050. One should recall that in 2003, the heat wave caused damage due to the shrinking and swelling of clay, for which compensation (via the natural disaster insurance scheme, and then via an exceptional compensation procedure for rejected cases) was estimated at approximately 1.3 billion € in Frécon and Keller (2009), while over the period 1989-2002, the average

90 annual cost of geotechnical drought for the natural disaster insurance scheme was more than five times smaller, with 205 million €.

Furthermore, subsidence is a risk with a long declaration period, with on average 80% of the number of claims declared two years after the event. This delay is due to the lengthy acceptance process of subsidence natural catastrophe declarations, upon which the validity of most claims is dependant. Although most insurers are reinsured against this peril with the CCR, the retention rate remains high (50%), it is thus necessary for insurers to develop their own view of this risk in order to estimate their exposure to this growing hazard. However, the inherent characteristics of subsidence make it a risk that is complex to model: it has slow kinetics and an absence of precise temporal definition, making subsidence models sparse on the market.

In 2007, plans (called PPR) for the Prevention of Differential Settlement Risks were prescribed in more than 1500 communes, as mentioned in Ministère de la transition écologique et solidaire (MTES) (2016). These plans are addressed in particular to anyone applying for a building permit, but also to owners of existing buildings. Its objective is to delimit the zones exposed to the phenomenon, and in these zones, to regulate the occupation of the land. It thus defines, for future construction projects and, if necessary, for existing buildings (with certain limits), the mandatory or recommended constructive rules (but also related to the environment near the building) aimed at reducing the risk of disorders appearing. In exposed sectors, the plan may also require a specific geotechnical study to be carried out, in particular prior to any new project. For the time being, therefore, these plans do not provide for d'inconstructibility. Among the advice given to minimize the risk of d'occurrence and l'ample of the phenomenon, there are instructions relating to the realization of a waterproof belt around the building, to the distance of vegetation from the building, to create a root barrier, to connect the water networks to the collective network, to seal the buried pipes, to limit the consequences of a heat source in the basement or to create a drainage device. There is also advice on how to adapt the building so as to counter the phenomenon and thus minimize the damage as much as possible, essentially by adapting the foundations (adopting a sufficient depth of anchorage, adapting according to the sensitivity of the site to the phenomenon, avoiding any dissymmetry in the depth of anchorage and preferring continuous and reinforced foundations, concreted to the full height of the excavation), by making the building structure more rigid (requiring the implementation of horizontal (top and bottom) (requiring the implementation of horizontal (top and bottom) and vertical (corner posts) ties for the connected load-bearing walls) or the disassociation of the various structural elements (by the installation of a rupture joint (elastomer) over the entire height of the building (including the foundations). building (including the foundations)).

Bevere and Weigel (2021) mention that since 2016, annual inflation-adjusted insured losses have continuously exceeded 600 million €, with an average annual loss close to 850 million which corresponds to around 50% of the CatNat premiums collected and makes subsidence possibly one of the most costly natural risk in France. Overall, a high to medium clay shrink-swell hazard affects one-fifth of metropolitan France's soils and 4 million individual houses, as mentioned in Antoni et al. (2017). And Soyka (2021) mentioned that this is not just in France, increased subsidence hazard gains attention in other countries, too (even if this article focuses solely on France).

1.3 Agenda

The purpose of this study is to provide a regression-based model that will allow to predict the annual frequency and severity of subsidence claims to be made, based on market data and climatic indicators. The model created in this study bases future

predictions on past occurrences, thus a historical insurance database was necessary to calibrate the models alongside indicators of the severity of historical events that could be reproduced into the future. These indicators were created using climatic and geological data that capture the specifics of past events and regional information. The creation of this database and the choice of indicators will be described in section 2. Using this historical data, various models are implemented, chosen to adapt to the particularities of the data in order to improve the precision of the predictions. There will be three layers to model the costs of subsidence claims (1) a drought event should be officially recognised (corresponding to a binary model, specificities of the French insurance scheme will be discussed in the next section) (2) if there is a drought, the frequency is considered (corresponding to a counting model, classically a Poisson model) (3) for each claim the severity is studied (corresponding to a cost model, here some Gamma model). As we will see, using so-called zero-inflated models, the first two models can be considered simultaneously. Various tree based models were also tested in an attempt to obtain more realistic predictions. In section 3, we will present those models, and we will analyse predictions obtained on the frequency, and more specifically discuss the geographical component of the prediction errors. And finally, in section 4, we will present some models to predict to total costs of subsidence events in France, and again, study mode carefully the prediction errors in 2017 and 2018.

2 Subsidence risk in France and our dataset

A yearly claim and exposure dataset, sourced from several different French insurers, relative to Multi-Peril Housing Insurance (*Multi-Risque Habitation*) for individual houses in metropolitan France for the period 2001 to 2018, was used here for frequency and severity of past events. This dataset was enriched with additional information based on geophysical indices usually used to model droughts.

Our dataset was aggregated at the town level[1] with no information about the particularities of each individual contract that could influence the claims (such as number of stories, size, orientation, etc.), creating the need for additional information about the climatic and geophysical exposure of a given town. One of the main issues when modelling subsidence is the absence of precise temporal and geographical definition of a subsidence events. Thus, to combat these issues, indicators must be created to grasp the geographical and temporal characteristics of past events.

In Section 2.1, after describing briefly the specificity of the French insurance scheme, we will explain the variables of interest we will model afterwards, namely the occurrence of a natural disaster (based on official data in France), the number of houses and building claiming a loss, and the amount of the losses (those last two based on data from three important insurance companies in France, with exposures spread throughout the country, representing about 20% of the French market). Then, in Section 2.2 and 2.3, we will describe possible explanatory variables (for the occurrence of a disaster, the percentage of houses claiming a loss and the severity). And finally, in Section 2.4 we discuss the use of other variables, mainly geophysical information since we want to predict subsidence, and not droughts in general.

---

[1] Here, we use here the word "*town*" to designate a "*commune*" (in French), or "*municipality*". There are 37,613 towns in metropolitan France (as characterized by their INSEE-"*commune*" code).

2.1 Specificity of the French *Catnat* system

The French "*Régime d'Indemnisation des Catastrophes Naturelles*" (also called the "CatNat regime") was created in 1982 (see Charpentier et al. (2021) for an historical perspective) although drought damages were added to the (informal) list of perils in 1989, as explained in Magnan (1995) or more recently Bidan and Cohignac (2017). The main idea of the mechanism is that any property damage insurance contract, for individuals as well as for companies, includes mandatory coverage for natural disasters. The assets concerned are buildings used for residential or professional purposes and their furniture, equipment, including livestock and crops, and finally motor vehicles. These assets are insured by multi-risk home insurance, multi-risk business insurance and motor vehicle insurance. The contractual guarantees (storm, hail and snow, fire...) are also very often attached to household and business contracts. Livestock outside barns and unharvested crops, on the other hand, are covered differently. It should be stressed here that the respective scope of insurable and non-insurable risks is not defined by law, but is established by case law. Indeed, the natural disaster insurance system is said to be "à péril non dénommé" (or unnamed peril) in the sense that there is no exhaustive list of all risks that are covered. The effects of natural disasters are legally defined in France as "*uninsurable direct material damage caused by the abnormal intensity of a natural agent, when the usual measures to be taken to prevent such damage could not prevent their occurrence or could not be taken*" (article L.125-1 of the insurance legal code). In practice (and it will be very important in our study) the state of natural disaster is established by an interministerial order signed by the Ministries of the Interior and of Economic Affairs. This order is based on the opinion of an interministerial commission. This commission analyzes the phenomenon on the basis of scientific reports and thus establishes jurisprudence regarding the threshold of insurability of natural risks. More specifically, in the context of our study regarding drought, requests for recognition of the state of natural disaster are examined for damage caused by differential land movements due to drought and soil rehydration. And a list of towns that have been declared a natural disaster are listed and associated guaranties are then applied, for both individual and commercial policyholders, by (private) insurance companies.

In comparison to other natural catastrophes, subsidence has certain particularities. From an insurance point of view, the typical event-based definitions of a natural catastrophe that is possible for cyclones or avalanches does not apply. Indeed, it has slow kinetics making it difficult to determine direct links of causality between the event and the claims. Damage can be caused long after the dry periods. However, that link of causality is the very definition of natural catastrophe recognition which makes the implementation of different criteria to determine the causality link of the event essential.

Subsidence was first observed as a major risk in France after the drought of 1976 which caused important damage to buildings. After a similar event in 1989, subsidence was integrated into the French natural catastrophe regime, in the sense that policyholders can claim a loss to their insurance companies. According to Mission des Risques Naturels (MRN) (2019), between 1989 and 2018, more than 11,300 towns have requested natural catastrophe recognition for subsidence and over 9,500 were granted it. The natural catastrophe declarations are published on average 18 months post-event, instead of 50 days for other natural catastrophes and the duration of an event is on average of 50 days for subsidence and of 5 days for other perils (like floods, avalanches or landslides, among many others). The total cost of subsidence losses reached 11 Billion € mid-2018, which is roughly 16,300€ per claim. The number of towns that have had their request declined has increased since 2003.

Overall, the proportion of acceptance is of 61%, however, just taking years subsequent to 2003, the proportion is of only 50%. As mentioned earlier, this might be explained by the fact that, according to the law, those events should be caused by "*the abnormal intensity of a natural agent* ". Thus, if a town is claiming losses every years, it ceases to be "*abnormal* ", and claims might be rejected then. Because the subsidence claim system is based on a 25 year return period threshold (as detailed in section 2.2), towns with recurring subsidence events would no longer be considered abnormal and their requests would be declined.

The evolution of the number of natural catastrophes since 1989, which is the year of the oldest natural catastrophe in the dataset, shows that since the 1990s the number of requests has been quite variable, however, 4 years seem to be abnormally hardly-hit: 2003, 2005, 2011 and 2018. Note finally that Wües et al. (2011) claims that since subsidence and drought are related to temperature, climate change will increase frequency and intensity of drought.

2.2   General considerations regarding drought indices

There exists many different options in terms of drought indicators to characterise their severity, location, duration and timing (see Svoboda and Fuchs (2016) for some exhaustive descriptions). The impact of droughts can vary, depending on the specificities of each drought, captured differently by each indicator. It is thus important to select an indicators with its application in mind. However, the availability of data also plays an important role in the selection, as it limits which indicator can be constructed.

The criteria to characterise the severity of shrinkage-swelling episodes evolved in 2018, as the old criteria were outdated and overly technical, making them difficult to interpret and explain to the public, see Ministère de l'intérieur (MI) (2019). The new system is based on two factors:

- **A geotechnical factor** pertaining to the presence of clay at risk of swell-shrink phenomenon, in place since 1989. This criterion enables the identification of soils with a predisposition to the phenomenon of shrinkage-swelling depending on the degree of humidity. The analysis is based on technical data established by the *Bureau des Recherche Géologiques et Minières* (BRMG), see Ministère de la transition écologique et solidaire (MTES) (2016). Areas of low, medium and high risk are considered to determine whether the communal territory covered by sensitive soils (medium and high-risk areas) is greater than 3%. This will be discussed in Section 2.4. However, the intensity of shrinkage-swelling is not only due to the characteristics of the soil but also to the weather.

- **A meteorological criterion** defined as a hydro-meteorological variable giving the level of moisture in superficial soils (1m of depth) at 8-kilometre precision level. This variable establishes the moisture of the soil for each season at a communal level called the Soil Water Index (SWI) which varies between 0 and 1, where 0 is a very dry soil and 1 is a very wet soil. A moisture indicator is calculated for every month, based on the average of the indicator of that month and the two previous months. This will be discussed in Section 2.2. For example, the indicator for July is fixed using the mean of the indexes for May, June and July, thus considering the slow kinetics of the drought phenomenon that can appear over a few months.

To determine whether a drought episode is considered abnormal, the SWI established for a given month is compared to the indicators for that same month over the previous 50 years. It is considered "*abnormal*" if the indicator presents a return period greater or equal to 25 years, as explained in Ministère de l'intérieur (MI) (2019). It should be stressed here that this return period is defined locally, and not nationally. If one of the months of a season meets the above criteria in a specific area, then the whole season is eligible to a natural catastrophe declaration for the entire town. If the natural catastrophe criteria are met and the Inter-Ministerial commission declares a subsidence natural catastrophe for the town, if the claims are in direct link with the event and the goods were insured with a property and casualty insurance policy then it will be covered by standard insurance policies. The presence of a threshold set at a 25-year return period indicates that over time, if a commune is regularly hit by extreme droughts, those events will be less and less likely to be declared natural catastrophes as they will lose their exceptional character.

However, over the years, the subsidence criteria have been changed and updated many times, to consider the new kinds of droughts that arose. The first main modification was in 2000, when a criterion based on the hydrological assessment of the soil was added to the criterion assessing the presence of clay in the soil which was the sole criteria before. However, 2003 was hit by an extreme and unusual drought limited only to Summer which was not captured by the criteria in place. Indeed, the uses of the criteria in place at the time would have led to most of the towns requesting a declaration to be refused. Thus, a new criterion was created specifically for 2003. In 2004, the criteria were updated once again, to consider droughts like that of 2003. However, in 2009 a new indicator was applied based on three seasonal Soil Water Indexes (SWI) (Winter, Spring and Summer) as well as the presence of clay in the soils. Finally, in 2018 the SWI criteria were updated to simplify the thresholds and create four seasonal indicators as presented previously and the shrinkage and swelling of clay exposure map was also updated.

2.3 Drought indices used as covariates

These indicators can be classed into three big families : The first are meteorological indicators, of which the most common amongst drought-related studies are the Standardised Precipitation Index (SPI), the Palmer Drought Severity Index (PDSI) and the Standardised Precipitation and Evapotranspiration Index (SPEI). These indices are based on precipitation data, as well as temperature and available water content for the two last ones. The SPI is the most widely used because it requires little data (only monthly precipitations needed) and is comparable in all climate regimes (see Kchouk et al. (2021) for a recent review of drought indices). However, those indexes do not capture drought through soil moisture, whereas other indexes such as Agricultural and Soil Moisture indicators do. Some common indicators from that family are the Normalised Difference Vegetation Index (NDVI), the Leaf Area Index (LAI) or the Soil Water Storage (SWS) which require more complex data such as spectral reflectance, leaf and ground area, soil type, available water content and more. Finally, the last smaller family of indicators are hydrological indexes, some examples of which are the Streamflow Drought Index (SDI), Standardised Runoff Index (SRI) or the Standardised Soil Water Index (SSWI) - which is used by Météo-France to characterise droughts and applied in the characterisation of soil dryness and climate change in (Soubeyroux et al. (2012)) - which require streamflow values, runoff information or soil water data.

Only a small portion of the above indicators could be considered given the limited data available. Indeed, the data used was
the monthly average water content, the monthly average soil temperature and the monthly average daily precipitations at a 9km
grid resolution globally, from the *ERA-5 Land* monthly database (Climate Change Service Climate Data Store (CDS) (2020)),
between January 1981 and July 2020. Therefore, only the SSWI and SPI were selected as they only require soil water content
and precipitation respectively and are simple to implement. Note that this SSWI, recently discussed in Torelló-Sentelles and
Franzke (2021), was inspired by Hao and AghaKouchak (2014) and Farahmand and AghaKouchak (2015).

The use of precipitation data alone is the greatest strength of SPI, as it makes it very easy to use and calculate. The ability
to be calculated over multiple timescales also allows SPI to have a wide scope. There are many articles related to SPI available
in the scientific literature, which gives novice users a wealth of resources they can count on for help. Unfortunately, with
precipitation as the only input, SPI is deficient when it comes to taking into account the temperature component, which is
important for the overall water balance and water use of a region. This drawback can make it more difficult to compare events
with similar SPI values, as highlighted in Svoboda and Fuchs (2016).

Similarly, the sole use of soil moisture, makes the SSWI a simple indicator to use but also a deficient one. However, as
pointed out in Soubeyroux et al. (2012), the SPI and SSWI are complementary : although they do have similarities, they show
some great difference. For example, they show that the droughts of 2003 are not linked to an extreme precipitation deficit:
Those droughts could not be detected through the SPI, but could be using the SSWI. In order to add an extra layer of detail
to better characterise droughts, a third indicator was created, based on the soil temperature available, inspired by the same
methodology as the SPI. In the rest of this article, it will be referred to as the standardised soil temperature index (SSTI).

To obtain indexes that are comparable all over France, the data must be transformed. Indeed, in its raw state, a dry period is
difficult to distinguish amongst a simply dry climate: the same magnitude of low precipitation in areas with very dry climates
will have a very different impact on the soil and on subsidence claims than in wet climates. The SPI methodology McKee et al.
(1993) allows the creation of normalised indicators (see also Guttman (1998) for a historical discussion). It is calculated using
3-month cumulative precipitation probabilities by calibrating a gamma distribution to the data, which is then transformed into
a standard normal distribution. Thus, it allows the quantification of the seasonal deviation of precipitation compared to the
historical mean. A three month step was chosen as it reflects short – and medium – term drought conditions and provides a
seasonal estimation.

In order to obtain indexes with the available data mentioned previously, the same methodology – which is the SPI compu-
tation methodology – was applied to the monthly average soil wetness, the monthly average soil temperature and the monthly
average daily precipitation separately, thus yielding the three-month SPI, SSWI and SSTI.

The aim of this study is to predict claims at a yearly time scale, creating the need for a yearly indicator. The 12-month sliding
SSWI, SPI or SSTI were not chosen as they would not capture the seasonality of droughts. Instead, to obtain yearly indicators

285 the extremes are taken over the 4 yearly seasonal indicators, with the following formulas[2]:

$$\text{ESSWI}_{z,t} = \min_{s \in \mathcal{S}} (\text{SSWI}_{s,z,t}), \tag{1}$$

$$\text{ESSTI}_{z,t} = \max_{s \in \mathcal{S}} (\text{SSTI}_{s,z,t}), \tag{2}$$

$$\text{ESPI}_{z,t} = \min_{s \in \mathcal{S}} (\text{SPI}_{s,z,t}) \tag{3}$$

where $\mathcal{S}$ denotes the set of seasons, $\mathcal{S} = \{\text{Spring}, \text{Summer}, \text{Autumn}, \text{Winter}\}$, $t \in \{1981, 1982, \cdots, 2020\}$ and z denotes the
290 given location. The ESPI is the Extreme Standardised Precipitation Index, the ESSTI is the Extreme Standardised Soil Temperature Index and the ESSWI is the Extreme Standardised Soil Water Index. This methodology – to our knowledge – has not been applied in the past for the creation of the soil temperature and precipitation indexes in the context of subsidence claim prediction.

(a) SSWI   (b) SPI   (c) SSTI
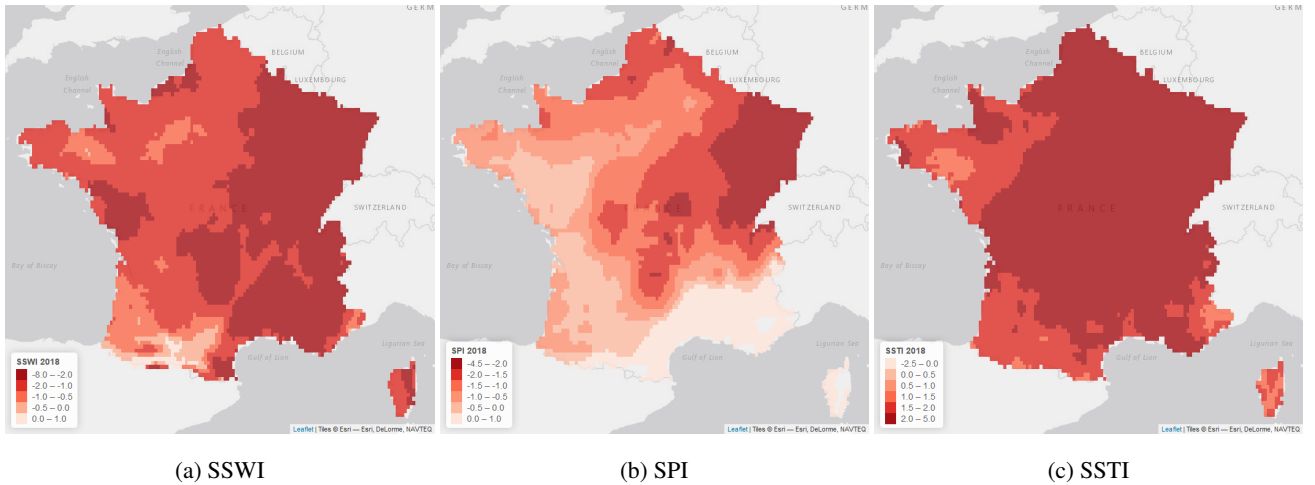
Figure 1. Indicators for 2018, with SSWI (Standardised Soil Water Index), SPI (Standardised Precipitation Index) and SSTI (Standardised Soil Temperature Index) from left to right.

2.4 Other spatial explanatory variables

295 The concentration and presence of clay in the topsoil plays an important role in the occurrence of subsidence as it is caused by the shrinkage and swelling of these particular kinds of soil. Thus, to express the risk of an area, a map was obtained from the Land Use and Cover Area Statistical Survey (LUCAS) database published by the European Soil Data Centre (ESDAC) (2015), which collects harmonised data about the state of land use and cover over the European Union. This map gives the concentration of clay in the topsoils (soils at 0-20cm depth) and is available at a 500m grid resolution over the European Union.

---

[2]Here, we use either the minimum or the maximum, depending if drought events are related either to low or high values of seasonal indices.

The soil clay concentration was then aggregated by town keeping the highest concentration of clay in the town, which gives the maps in figure 2a. Other aggregation functions were considered (such as the average), but they were less predictive than the maximum. This map shows that the areas with the highest clay concentrations appear to be in the North-East of France, in Charente-Maritime (West), around Toulouse (South-West) and along the Mediterranean Sea (South-East).

Finally, a binary categorical variable, which takes the values 1 if the town has historically made a request for a natural catastrophe declaration and 0 otherwise, was sourced from CCRs' historical data, CCR [2020]. The risk map obtained is visible in figure 2b, as at 2018.
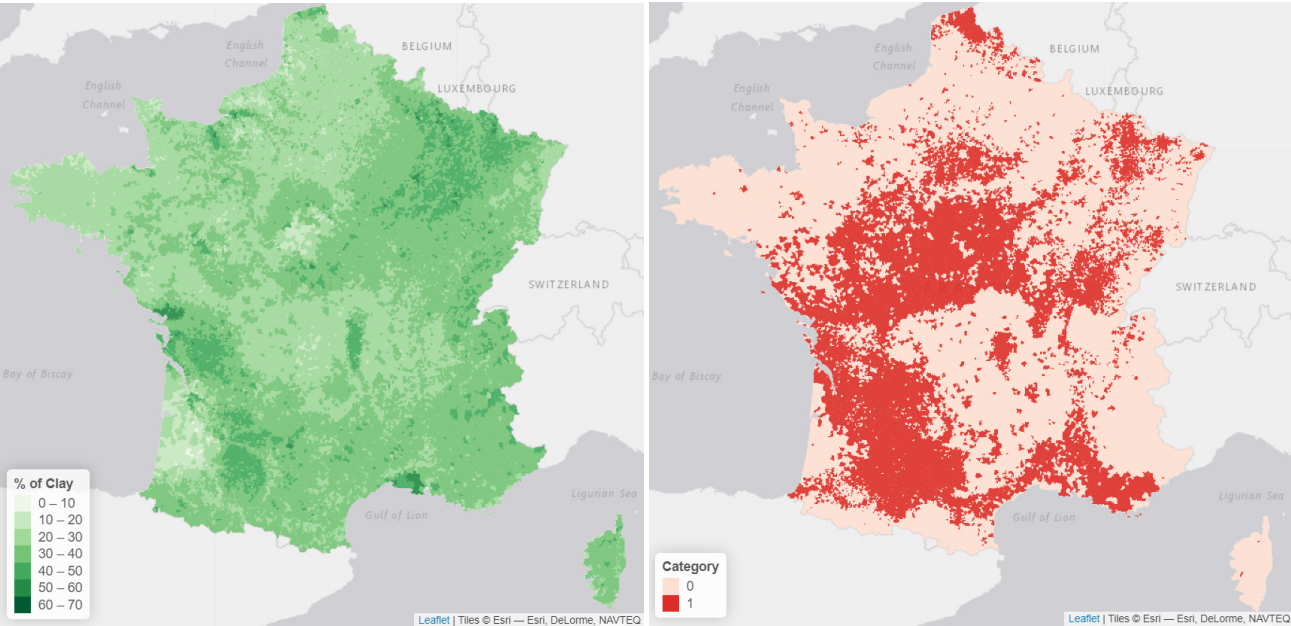
(a) Topsoil clay concentration   (b) Natural catastrophe occurence

Figure 2. Topsoil clay concentration and historical natural catastrophes accepted requests. Those two variables will be used for our predictive model.

These variables were then aggregated to the exposure dataset. Thus, the calibration dataset was composed for each claim year of the "INSEE code" of the town (from the official classification, that can be seen as the ZIP code used in the U.S.), the year of the claim, the number of claims, the cost of claims (in €), the number of policies, the total sums insured (in €), the clay concentration in the soil, the ESPI, the ESSTI, the ESSWI and Cat (the binary categorical variable giving the occurrence of a historical natural catastrophe declaration request, prior to the year of study). All the models calibrated are based on those five variables mentioned above.

3 Model calibration for the frequency

At regional scale, Corti et al. (2009, 2011) pointed out that it is possible to use simulations to get a good representation of the regions affected by drought-induced soil subsidence, but substantial differences between simulated and observed damages in some regions remain. In this section, we will describe a simple spatio-temporal model for resilience, to model either the frequency or the intensity of such events (on a yearly basis). Regression type models will be considered as in Blauhut et al. (2016). The main difference is that the interest was to model occurrence, and a logistic regression was sufficient. Here, since we focus on frequency and intensity, some Poisson-type regression models will we considered first, and then some Gamma models for the severity, to predict the economic cost of subsidence. In Section 3.3 we will present regression based models, that we will extend in Section 3.4 to ensemble models, namely with bagging of regression trees, as suggested in Breiman (1996) to take into account some possible non-linearity as well as cross-effects. And in section 3.5, we will study more carefully the errors. But before, we need to introduce some criteria to select an appropriate model.

3.1 Model selection criteria

Various validation performance measures are used to compare the different models. They are chosen to optimise the model selection based on the qualities that are desired from the model which are: a good capacity at predicting the correct number of claims in the right areas, the ability of not predicting claims where there are none historically all the while keeping the simplest possible model. The following performance measures are thus used:

- Akaike Information Criteria (AIC) and Bayesian Information Criteria (BIC), which use maximum likelihood and penalises models with respectively too many variables and too many variables with respect to the number of observations. These criteria are only used for the parametric regression models.

- Root Mean Square Error (RMSE) – or simply the sum of the squares of errors, which penalises greatly extreme errors, i.e. extreme deviations in predictions. This will be used for costs, and not counts.

3.2 Cross-Validation method

In order to assess the predictive power of the calibrated models, cross-validation was used. The main goal of the models is to predict accurately the number of claims per town on a yearly basis, thus a yearly cross-validation that is derived from the basic cross-validation principle will be used.

The idea of cross validation is related to in-sample against out-of-sample testing. In a nutshell, the model is fitted on a subset of the data, and validation is computed on observations that were left out. This approach is interesting to assess how the results of some statistical analysis will generalize to an 'independent' data set. Note that it is possible to remove one single observation, and to validate the model on that one – this is the *leave-one-out* approach – or to split the original dataset on k subgroups, to remove one subgroup to fit a model, and predict on that specific subgroup, and rotate – this is the *k-fold cross-validation* approach. In the case of spatio-temporal data, two approaches can be used,

- use some regions as subgroups, then use some spatial k-fold approach (as in Pohjankukka et al. (2017)) where the model is fitted on $k-1$ regions, and validation is based using some metric on the error on the region that was left out – it can be the sum of the squares of the difference, or any metric discussed in the previous section,

- use cross-validation in time, but because of particular properties of the *time* dimension, cross-validation is performed by removing the future from the analysis (as in Bergmeir et al. (2018)): at time t, we use observations up to time t to fit a model, then get a prediction for time $t+1$. In some sense, it is a classical leave-one-out procedure, except that we cannot use observations *after* time $t+1$ to get a prediction at time $t+1$. This approach is used in this study.

3.3 Regression-based models

A first attempt at modelling the yearly number of claims was made using Generalised Linear Models (GLM) with Poisson, Binomial and Negative Binomial distributions, which are the most adapted to the calibration data (on counts). These models offer a simple and interpretable approach to model data by assuming that the response variable $\boldsymbol{Y} = (Y_{z,t}) \in \mathbb{R}^{n \times T}$ is generated by a given distribution and that its mean is linked to the q explanatory variables $\boldsymbol{X} = (\boldsymbol{X}_{z,t}) \in \mathcal{X}^{n \times T}$ (where classically $\mathcal{X} = \mathbb{R}^q$), through a link function. In this model, we have n spatial locations (the number of towns), T dates (the number of years), and q possible explanatory variables.

If we want to model the number of houses claiming a loss in a given location, the Poisson GLM is defined as $Y_{z,t} \sim \mathcal{P}(E_{z,t} \cdot \lambda_{z,t})$, for a location z and a year t, where $E_{z,t}$ is the exposure (the number of contracts in the town) and $\lambda_{z,t}$ is the yearly intensity, per house,

$$\lambda_{z,t} = \exp\left[\beta_0 + \beta_1 x_{1,z,t} + \cdots + \beta_k x_{q,z,t}\right] \tag{4}$$

where $x_{j,z,t}$'s are features used for modeling, such as the ESSWI, the ESSTI, etc. The prediction, performed at year $t+1 \in \{2001, ..., 2019\}$ based on a calibration set of years $\{2001, ..., t\}$, is

$$_t\widehat{N}_{z,t+1} = E_{x,t+1} \cdot {}_t\widehat{\lambda}_{x,t+1} \tag{5}$$

and, based on estimator $\widehat{\boldsymbol{\beta}}_t$ obtained on the training dataset with observations of years $\{2001, ..., t\}$, using maximum-likelihood techniques, and

$$_t\widehat{\lambda}_{z,t+1} = \exp\left[\widehat{\beta}_{0,t} + \widehat{\beta}_{1,t} x_{1,z,t+1} + \cdots + \widehat{\beta}_{k,t} x_{q,z,t+1}\right] \tag{6}$$

where geophysics covariates $x_{j,z,t+1}$ are known. In Table 1 several sets of parameters estimates $\widehat{\boldsymbol{\beta}}_t$ are given (with t varying from 2008 until 2018).

From Table 1, we can see that the model is rather stable over time, which is an interesting feature from a modeler's perspective: if we predict more claims due to subsidence in time, it is mainly due to the underlying factors than to the change in the impact of each variable. It can be mentioned that $\widehat{\beta}_{3,t}$ (associate the clay) is significantly increasing (with a p-value of 2%).

This Poisson model is rather classical to model counts, and it is said to be an equi-dispersed model, in the sense that the variance of Y is equal to the average value. This model can be extended in two directions, instead of having

Table 1. Evolution of the parameters in the regression (Poisson regression). Numbers in brackets are the standard deviations of the parameters. Note that two ESSPI parameters are not significant here (95% level).

year	t	2008	2010	2012	2014	2016	2018
Intercept	$\widehat{\beta}_{0,t}$	-13.668	-13.460	-13.522	-13.735	-13.932	-14.357
		(0.074)	(0.071)	(0.062)	(0.06)	(0.059)	(0.049)
ESSTI	$\widehat{\beta}_{1,t}$	1.522	1.420	1.511	1.494	1.539	1.661
		(0.017)	(0.015)	(0.013)	(0.013)	(0.013)	(0.012)
ESSWI	$\widehat{\beta}_{2,t}$	-0.711	-0.700	-0.601	-0.709	-0.750	-0.707
		(0.011)	(0.011)	(0.009)	(0.009)	(0.009)	(0.008)
clay	$\widehat{\beta}_{3,t}$	0.021	0.020	0.024	0.025	0.025	0.035
		(0.001)	(0.001)	(0.001)	(0.001)	(0.001)	(0.001)
cat	$\widehat{\beta}_{4,t}$	3.924	3.950	3.957	3.957	4.003	3.902
		(0.056)	(0.055)	(0.049)	(0.048)	(0.047)	(0.038)
ESSPI	$\widehat{\beta}_{5,t}$	-0.046	-0.010	0.016	0.074	0.127	-0.048
		(0.013)	(0.011)	(0.009)	(0.009)	(0.009)	(0.007)

- the binomial model, where $Y_{z,t} \sim B(E_{z,t}, p_{z,t})$, where $E_{z,t}$ is the exposure and $p_{z,t}$ is the probability that, for a given year t and location z, a claim is made for a single house, and the prediction for $p_{z,t+1}$ is

$$
{}_t\widehat{p}_{z,t+1} = \frac{\exp\left(\widehat{\beta}_{0,t} + \widehat{\beta}_{1,t}x_{1,x,t+1} + \cdots + \widehat{\beta}_{k,t}x_{q,x,t+1}\right)}{1 + \exp\left(\widehat{\beta}_{0,t} + \widehat{\beta}_{1,t}x_{1,x,t+1} + \cdots + \widehat{\beta}_{k,t}x_{q,x,t+1}\right)} \tag{7}
$$

In that case, we have an under-dispersed model in the sense that by construction we must have $\mathrm{Var}[Y_{z,t}] < \mathbb{E}[Y_{z,t}]$

- the negative binomial model, where $Y_{z,t} \sim NB(E_{z,t}, p_{z,t})$, where $E_{z,t}$ is the exposure and $p_{z,t}$ is the probability, with standard notations for the negative binomial probablity function. In that case, we have an over-dispersed model in the sense that $\mathrm{Var}[Y_{z,t}] > \mathbb{E}[Y_{z,t}]$

Calibrating the GLMs and averaging the indicators over the years spanning from 2001 to 2018 and using the yearly cross-validation method, the results on the left of Table 2 were obtained. This table shows that the Negative Binomial model has the lowest AIC and BIC.

In order to better consider the characteristics of the claims data, Zero-Inflated models were tested using Poisson and Negative-Binomial distributions. In these models the joint use of logistic and count regression allows the integration of the over-representation of non-events in the data. More formally, in Zero-Inflated models, given a location and a time (z, t), we assume that there is a probability of having 0 claims. In our context, it could mean that the town has not been recognized as hit by a drought event. The occurrence of a drought is modeled with a logistic model with probability $p_{z,t}$ here. Then, if there is a drought event, the number of claims is driven by some specific distribution (Poisson, Binomial, or Negative Binomial), as

introduced by Lambert (1992). If we consider a Poisson regression it means that

$$\mathbb{P}(Y_{z,t} = 0) = p_{z,t} + (1 - p_{z,t})e^{-\lambda_{z,t} \cdot E_{z,t}} \tag{8}$$

(the second part comes from the fact there there could be a drought, but the number of counts of claims is null) and

$$\mathbb{P}(Y_{z,t} = y) = (1 - p_{z,t})\frac{[\lambda_{z,t} \cdot E_{z,t}]^y e^{-\lambda_{z,t} \cdot E_{z,t}}}{y!}, \text{ where } y = 1, 2, 3, \cdots \tag{9}$$

where $\lambda_{z,t}$ and $p_{z,t}$ are related to covariates through expressions as Equation (4) and (7), respectively. Note that such models can easily be estimated with standard statistical packages. The results of the Zero-Inflated models are visible on the right of Table 2. It shows that the Zero-Inflated Negative-Binomial model is better than the Zero-Inflated Poisson model.

Table 2. Quality measures for the different GLM distributions.

	Binomial	Poisson	NB	zero-inflated	
				Poisson	NB
AIC	115,051	114,189	100,491	71,154	54,375
BIC	115,113	114,252	100,564	71,259	54,510

Figure 3 shows the yearly predictions for the zero-inflated models, alongside the previously tested GLMs[3].

When looking at the yearly total predictions compared to reality, as observed in figure 3, all the GLM predictions are very similar apart from the negative binomial model which overpredicts (massively) in 2018, however they all overestimate claims in 2018 and underestimate the number of claims in 2003, 2011, 2016 and 2017. This graph shows that the predictions closest to the reality line are for the Negative-Binomial Zero-Inflated model. That model also has the best metrics when comparing to those of the GLMs. Thus, Zero-Inflated models appear to provide a better fit than the GLMs.

This section showed that the Zero-Inflated models, in particular the Negative-Binomial Zero-Inflated model, outperformed the GLMs in terms of number of claims and model selection criteria. In the next section, we will see the alternatives to regression-type models that can be considered, since the "*linear model*" assumption might be rather strong here.

3.4 Tree-based models

Tree-based models are popular models for data analysis and prediction and offer an alternative to the previous parametric models. Popularised by Breiman et al. (1983), regression trees produce simple and easily interpretable split rules.

– A Regression Tree is such that

$$_t\widehat{Y}_{z,t+1} = \sum_{\ell=1}^{L} \widehat{\omega}_{\ell,t} \mathbf{1}(\boldsymbol{x}_{z,t+1} \in \mathcal{L}_\ell) \tag{10}$$

---

[3]For purposes of confidentiality, the total number of claims per year are withheld, but the proportions on the y-axis are valid.
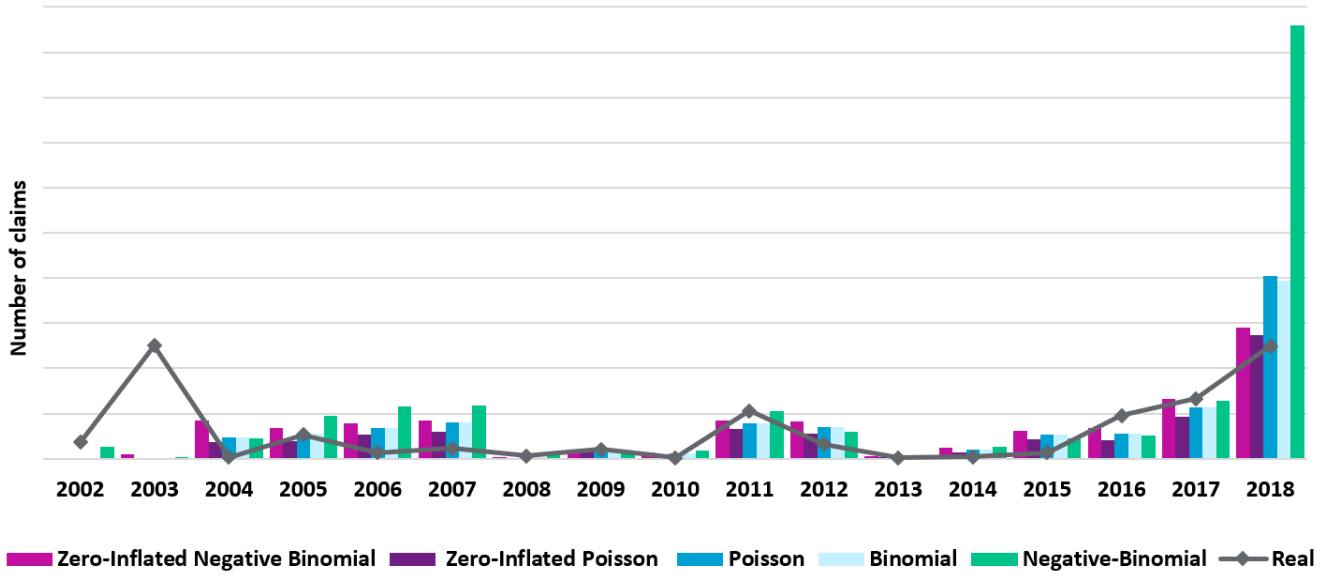
Figure 3. Yearly predictions for the Zero-Inflated models and GLMs

where $\{\mathcal{L}_1, \cdots, \mathcal{L}_L\}$ is a partition of $\mathcal{X}$, and $\mathcal{L}_j$'s are called *leaves*. In a tree with two leaves, $\{\mathcal{L}_1, \mathcal{L}_2\}$, there is a variable j such that $\mathcal{L}_1$ is the half-space of $\mathcal{X}$ characterized by $x_{j,t} \leq s$ while $\mathcal{L}_2$ is characterized by $x_{j,t} > s$ for some threshold s. For the "classical" regression tree, the split is based on the squared loss function, in the sense that we select s to maximise the between-variance, or equivalently, minimise the within-variance. It is possible to extend this approach by using, instead of the squares of residuals (corresponding to the squared loss function), the opposite of the log-likelihood of the data. This can be performed using the `rpart` R package (see Breiman et al. (1983) for further details on regression trees).

If trees are simple to interpret, they are usually rather unstable: when fitting a tree on a subset of observations, it is common to get different splitting variables, and therefore different trees. The idea of *bagging* (as defined in Breiman (1996)) is to use a boostrap procedure to create samples (re-sampling the observations with replacement) and then aggregate predictions. In the case where the number of covariates is not too large, this is also called a Random Forests, from Breiman (2001).

Two Tree-Based models are tested here, in order to attempt to improve the previous predictions :

– A "classical" Random Forest (RF),

$$_t\widehat{Y}_{z,t+1} = \frac{1}{m}\sum_{i=1}^{m} {}_t\widehat{Y}_{z,t+1}^{(i)} \text{ where } {}_t\widehat{Y}_{z,t+1}^{(i)} = \sum_{\ell=1}^{L_i} \widehat{\omega}_{\ell,t}^{(i)} \mathbf{1}(\boldsymbol{x}_{z,t+1} \in \mathcal{L}_\ell^{(i)}) \tag{11}$$

where each tree – corresponding here to different i's – is computed using a squared loss function, on different boostrap samples (obtained by resampling n observations, with replacement, out of the initial n ones). This can be performed using `randomForest` R package.

430 – A Poisson Random Forest (RFP) which considers count data, with the aim of better capturing the distribution of the data. Poisson Random Forests are a modified version of Breiman's Random Forest allowing the use of count data with different observation exposures. This is done by modifying the splitting criterion so that it maximises the decrease of the Poisson deviance. An offset has also been introduced to accommodate for different exposures. This Random Forest was calibrated using the `rfPoisson` function available in the `rfCountData` package in R.

435 These Random Forests were all tuned in order to obtain optimal number of trees, number of variables tested at each split and maximum number of nodes. However, the tuning was limited given the length of the tuning process, which may reduce the quality of the models.
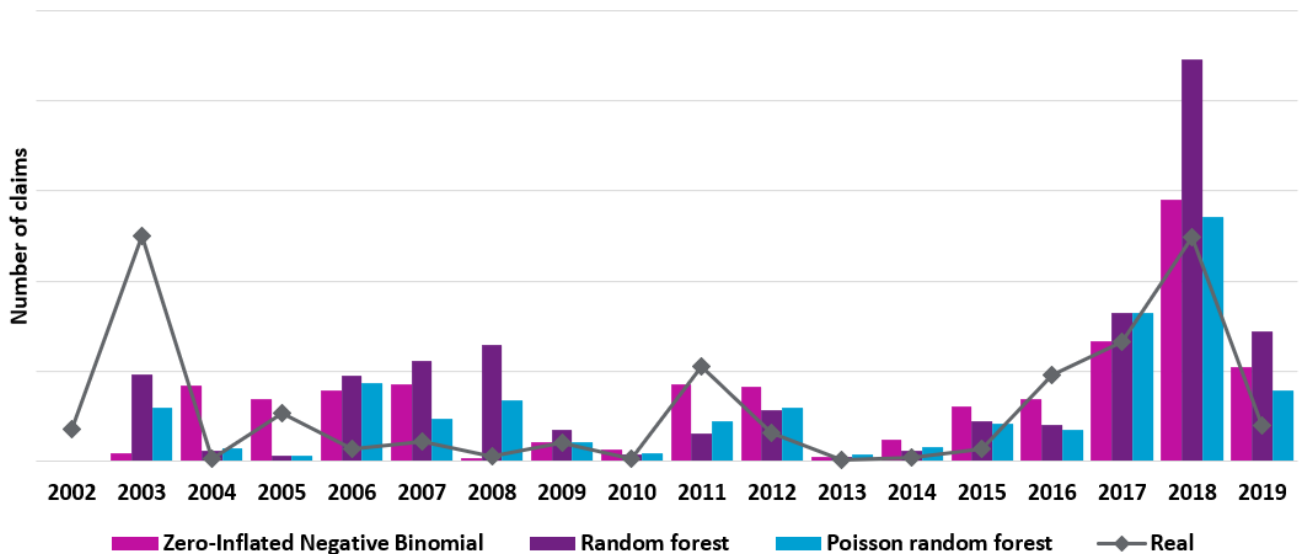
Figure 4. Comparison of yearly predictions for the tree-based models, with ZINB, classical RF, and RFP.

The figure 4 shows the total yearly predictions for each tree-based model alongside the Zero-Inflated Negative Binomial model and the real claims. It shows that the closest predictions to the real observations (the plain line) seem to be those of 440 the Zero Inflated model and the Poisson Random Forest, although all models but the Zero-Inflated model underestimate 2011 and 2016. With our cross-validation approach, we have poor results for early years (only data from 2002 were used to derive a model for 2003). The standard Random Forest overpredicts 2018.Thus, the Zero-Inflated model and the Poisson Random Forest appear to have the best predictions.

Through this section, two different Random Forests were presented; however, the one with the best results is the Poisson Random Forest which rendered similar results as the Negative-Binomial Zero-Inflated model. The complex calibration process and the unclear influence and importance of the variables on the output of the Poisson Random Forest make it a less attractive choice of model compared to the Zero-Inflated regression, which has a clear variable influence and a simple prediction formula. One can thus wonder whether such a loss in interpretability is worth such a small gain in terms of predictions.

3.5 Mapping the predictions

In order to improve the predictions, and only predict the actually impacted areas, a methodology was developed to optimise the removal of all the very low claim predictions. This methodology was applied to both the Zero-Inflated model and the Poisson Random Forest. The total predictions changed little, and the geographical distribution of both models' predictions are observable for 2018 in figure 5.

In 2018, both models have more or less the same claim distribution, with large amounts of claims along the Mediterranean, in the North and in Pays-de-la-Loire. However, the distribution is slightly different when looking at the centre of France. Indeed, the Random Forest seems to predict more claims in that area than the Zero-Inflated Negative Binomial model. Comparing these results with the real claims for 2018, it can be seen that the historical claims are nearly exclusively concentrated in the centre of France with a few claims along the Atlantic and Mediterranean coast and in the North-East of France. Thus, both models seem to over predict the claims around the coasts of France and – slightly for the Poisson Random Forest and vastly for the Zero-Inflated Negative Binomial model – under-predict in the centre of France. However, it can be noted that the over-predicted areas do mostly fall within areas that have non-recognised natural catastrophe declarations which could mean that the area was hit but not compensated and thus that the models have difficulty assessing the difference between areas that will be recognised as natural catastrophes or not. The same conclusion can be made when looking at the predictions for 2017, visible in figure 6.

In these maps, the predicted claims do appear to be in the correct areas in the South and South-West of France for both models, however, there are overpredictions in the East, centre and North of France, which also appear to be areas with non accepted natural catastrophe declarations. Both models seem to predict the correct areas but also additional zones that often are areas that have refused natural catastrophe declarations, which means that those areas were impacted by subsidence but not sufficiently to enter into the scope of the natural catastrophe regime. Indeed, as the acceptance criteria changed frequently between 2001 and 2018, the models cannot capture the natural catastrophe aspect of a claim seeing as one that may have been acceptable in 2017 may no longer be today. Both models predict more or less the same geographical distribution of claims, posing the question of the usefulness and practicality of using a complex model such as the Poisson Random Forest compared to the Zero-Inflated Negative-Binomial model.

Another option that would permit the classification of the predicted claims into accepted and refused natural catastrophe categories, would be to use the Shrinkage and Swelling of clay risk map Georisques (2020), published by Geological and mining research bureau (BRGM). This map categorises the exposure of a given point of France between four categories: not at risk, low risk, average risk and high risk. The acceptance of a natural catastrophe declaration in France is feasible if more
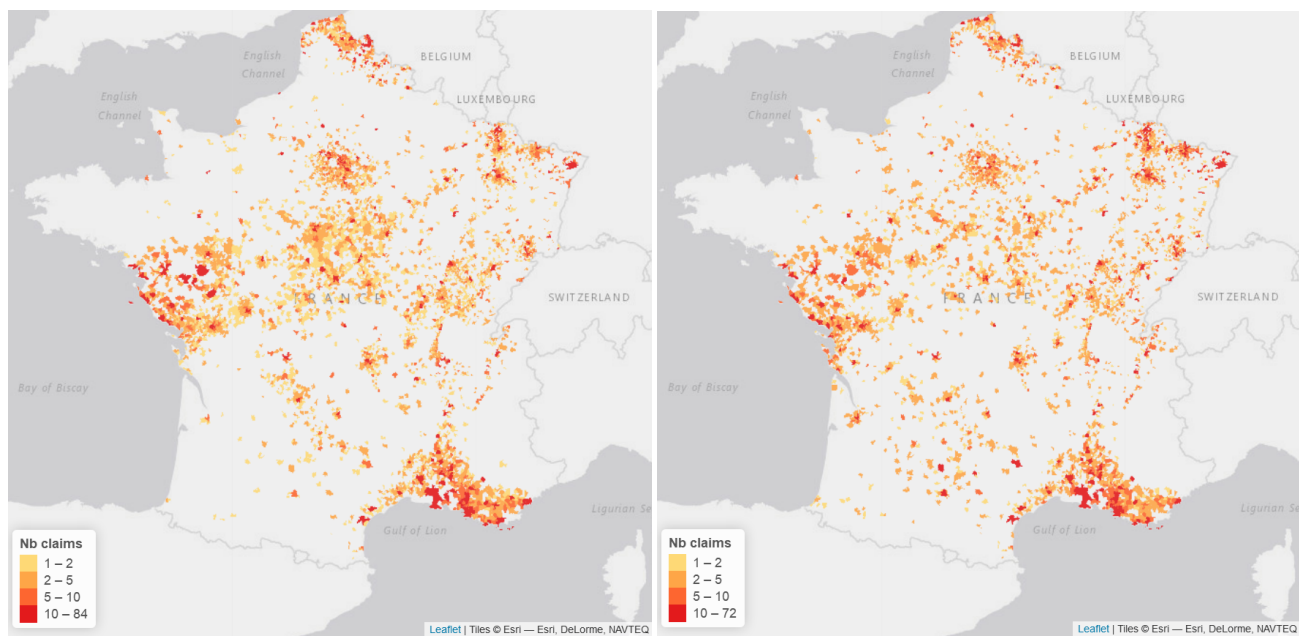
(a) Poisson RF

(b) Zero-Inflated
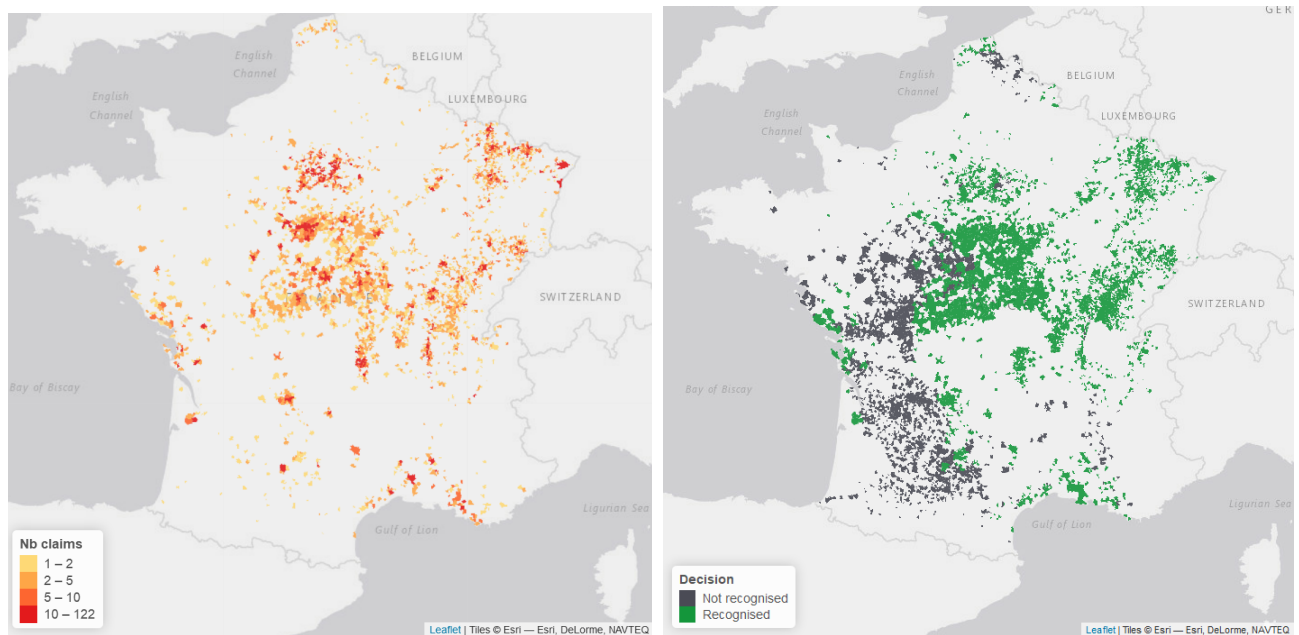
(c) Observed claims

(d) Nat.Cats.

Figure 5. Observed and Predicted number of claims for 2018

(a) Poisson Random Forrest (RFP)

(b) Zero-Inflated (ZINB)

(c) Observed claims

(d) Nat.Cats.
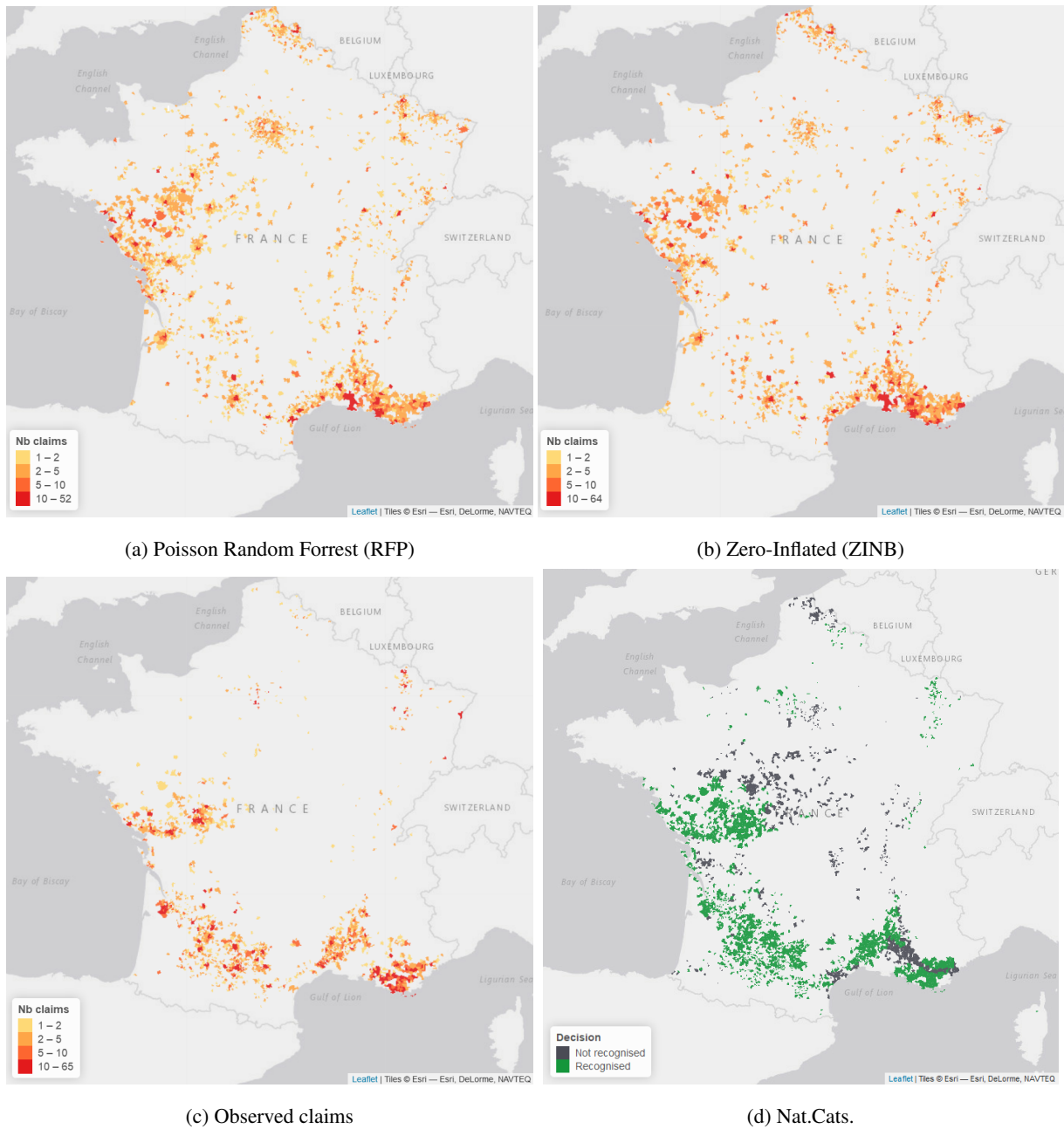
Figure 6. Observed and Predicted number of claims for 2017

than 3% of the surface of a town is in a zone with average or high risk. Thus, if the predicted claims map and the risk map, aggregated by town, were overlapped, the classification of the predicted claims would be possible between potentially accepted and most likely refused natural catastrophe declaration.

4 Cost predictions

In the previous section, we saw different models used to predict the frequency (the number of claims per town). Here we consider a Gamma model for the average cost per claim, leading us towards a *compound model* for the total cost per town, as introduced in Adelson (1966), and used for example in hydrology in Revfeim (1984) or Svensson et al. (2017), or for droughts in Khaliq et al. (2011).

4.1 Modeling average and total economic costs

For a given location z and year t, the total cost (from the insurer's perspective) is a *compound sum*, in the sense that

$$Y_{z,t} = \sum_{i=1}^{N_{z,t}} Z_{i,x,t} = \begin{cases} Z_{1,x,t} + \cdots + Z_{N_{z,t},x,t} \text{ if } N_{z,t} > 0 \\ 0 \text{ if } N_{z,t} = 0, \end{cases} \tag{12}$$

with a random sum of random costs. Here $N_{z,t}$ is the frequency, modeled in the previous section, and $Z_{i,x,t}$'s are individual economic losses per house. It is possible to consider here a Tweedie GLM, as introduced in Jørgensen (1997), corresponding to a compound Poisson model, with Gamma average cost. Nevertheless this is only a subclass of the general compound models. Note that Tweedie models are related to a *power-parameter*, since they are characterize by the relationship $\mathbb{E}[Y] = \text{Var}[Y]^\gamma$. If $\gamma = 1$, Y is proportional to a Poisson distribution (average costs are non-random), while $\gamma = 2$ means that Y is proportional to a Gamma distribution (frequency is non-random). For inference, we used $\gamma = 1.5$ which corresponds the lowest AIC. For the corresponding Tweedie model, SSTI, SSWI, as well as Clay and Cat covariates were used.

Although the model is interesting, it is less flexible than having two separate models one for the frequency, and one for the average cost at location z, for year t, written

$$Y_{z,t} = N_{z,t} \cdot \overline{Z}_{x,t} \tag{13}$$

where (as before) $N_{z,t}$ is the frequency, as modeled in the previous section, and the average cost (per house) is modeled using our data, aggregated at the town level, $\overline{Z}_{x,t}$. The prediction is then

$$_t\widehat{Y}_{z,t+1} = {}_t\widehat{N}_{z,t+1} \cdot {}_t\widehat{Z}_{z,t+1} \tag{14}$$

The results of these methods are rather similar. Figure 7 shows the total yearly predictions for the Tweedie model and the average cost of claims method using the GLM and both the Zero-Inflated and Poisson Random Forest models, previously calibrated.

Figure 7 shows that the Tweedie model makes predictions that are similar to the previous cost of claims predictions, however this model over-estimates less the year 2018 and (clearly) over-estimates more the years 2007 and 2012. On the other hand, the years 2003, 2011 and 2016 are still severely underestimated by the three predictions, although less so by the Tweedie model.
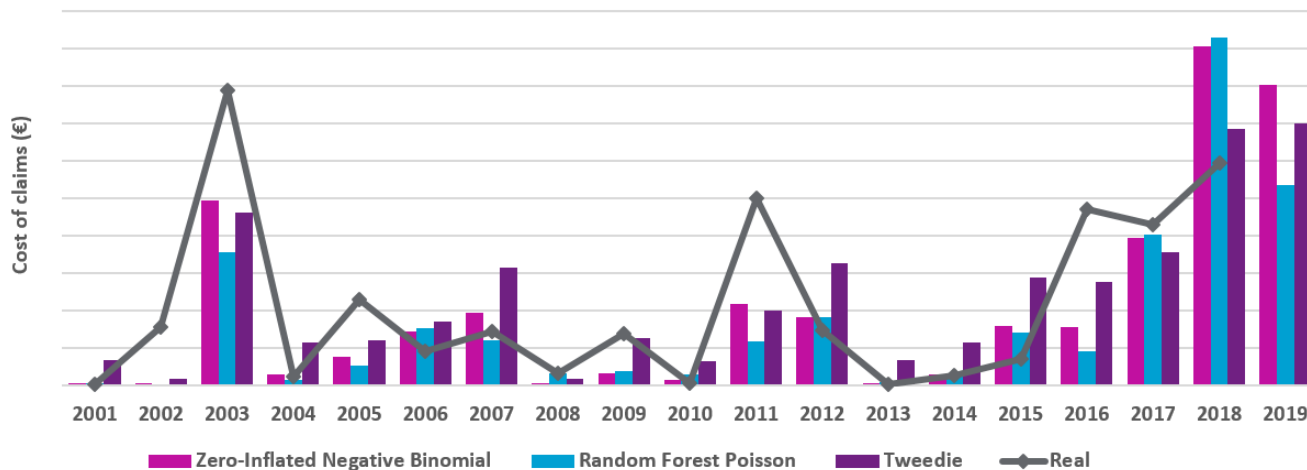
Figure 7. Total yearly cost predictions in France, with a ZINB model + Gamma costs, RFP model + Gamma costs, and a Tweedie model (Poisson + Gamma costs).

4.2 Mapping the predictions

As in section 3.5, it is possible to visualize the prediction, and to map $_{2016}\widehat{Y}_{z,2017}$ and $_{2017}\widehat{Y}_{z,2018}$, in Figure 8. As expected, if we are not able to predict correctly the frequency, the cost is overestimated. Overall (as we can see on Figure 7), in 2017, we obtained a good prediction in France, but we can observe some spatial differences. Most of the comments made in section 3.5 remain valid, and clearly, predicting the economics losses in a specific area is not a simple task.

In this study, we considered to forecast claims for time $t+1$ based past data up to time t, and climatic varaibles for time $t+1$. Therefore, it is not possible to forecast claims in the future, since we would have to get forecasts of future climate dataset for all three climatic indicators (ESSTI, ESSWI and ESPI) using the soil wetness, soil temperature and precipitation data in different RCP scenarios and use these new future climate indicators to estimate the impact of climate change on future claims in each scenario. Furthermore, one must keep in mind that the results would be base on todays' legal environment and are barring any evolution in the way subsidence claims are covered. This methodology would also be flawed by the generally larger granularity of future climate data, which renders the estimation less precise (eg. CMIP5 future climate data[4]) which has lower resolution compared to ERA5 land data used in this study).

5 Conclusions

The increase in number and severity of subsidence claims in the past years has created a need for insurers to improve their grasp of the knowledge of this risk. However, the implementation of subsidence models is time consuming and requires detailed

---

[4]https://cds.climate.copernicus.eu/cdsapp#!/dataset/projections-cmip5-monthly-single-levels?tab=overview
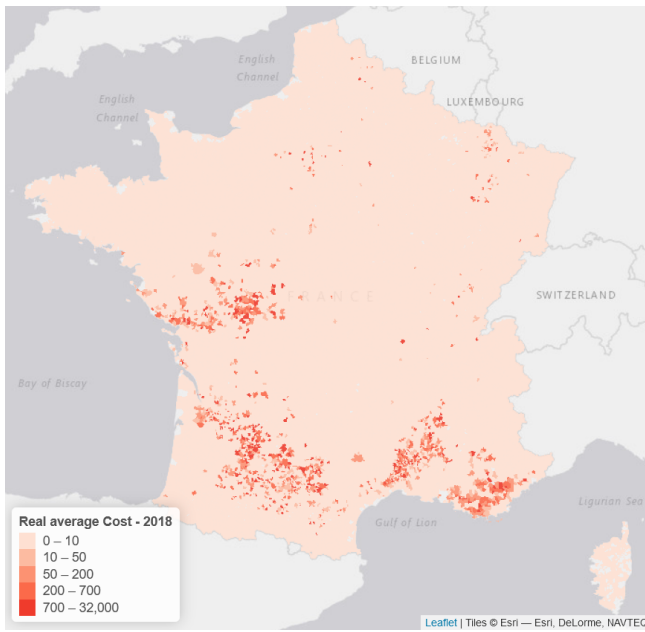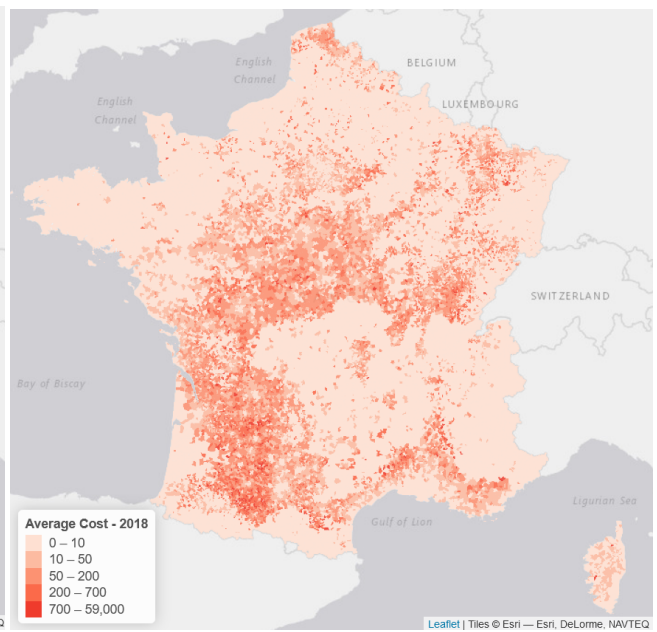
(a) Real 2017

(b) Predicted 2017
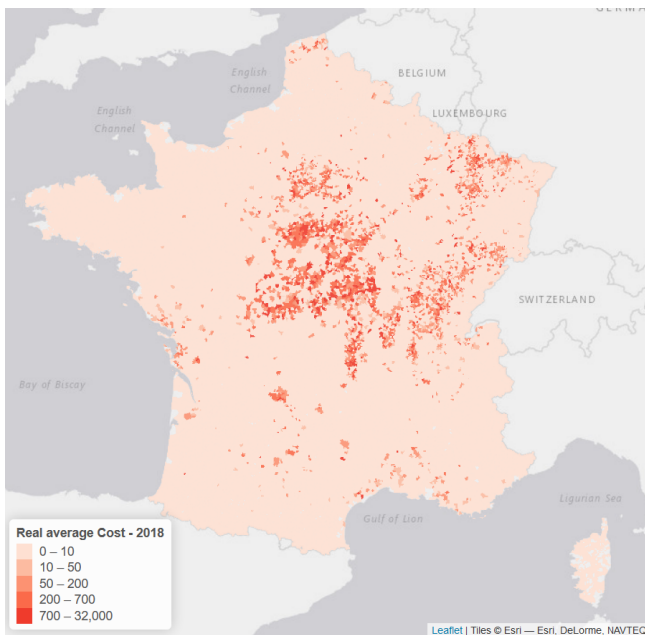
(c) Real 2018
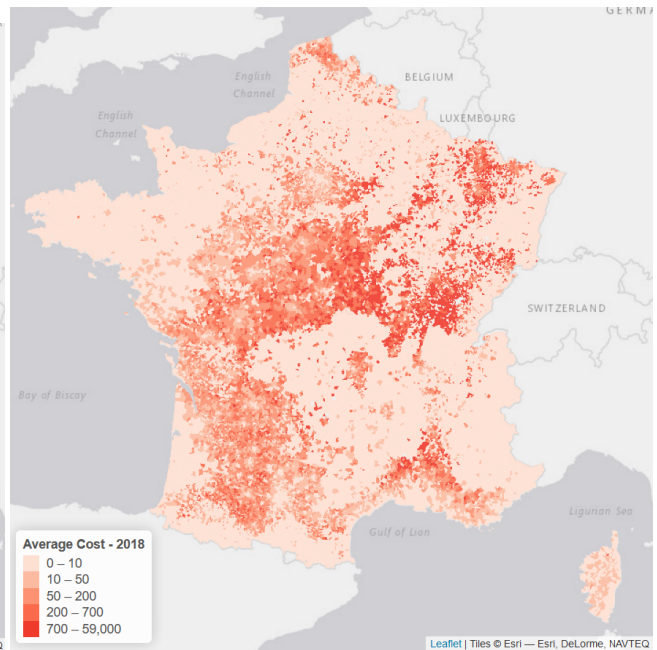
(d) Predicted 2018

Figure 8. Observed and Predicted average cost of claims in 2017 and 2018

data. This study proposed a method of approaching the costs and frequency of claims due to subsidence based on historical data. This was applied through two main components: the development of new drought indicators using Open Data and the use of parametric and tree-based models to model this risk. Modelling subsidence requires the integration of meteorological and geological indicators to ascertain the factors predisposing a policy to subsidence. Without this information, the inherent risk to which a dwelling is exposed cannot be perceived. For this reason, geological and meteorological data was obtained from Open Data sets. This data was paired with insurance exposure and claim data to obtain a complete dataset used to calibrate the models. However, the data available was only at a communal mesh, making the results less precise. Indeed, subsidence is a very localised risk whose modelling would benefit from policy level data.

Overall, the methods enable the predictions of an estimate of the number of claims, cost of claims and their geographical distributions. Although they sometimes lack in precision, the models give a good indication of the severity of a given year. The uncertainty in the predictions may be explained by the non-homogeneous data on which the models were calibrated. Indeed, the natural catastrophe declaration criteria evolved many times over the calibration period, rendering the historical data biased. The predictions would also have benefited from data at a finer mesh to take into account the individual particularities of each policy such as the presence of trees close to the construction, the slope of the terrain, the orientation of the slope, etc. Finally, more precise temporal definition of the events could have been used if the claims were available at a monthly scale rather than yearly. In that case, seasonal indicators could have been created, rather than yearly ones, to capture more precisely the time scale of an event.

This study has allowed for the creation and implementation of new drought indicators for a subsidence claim model which performs well considering the limitations induced by the lack of information and precision of the calibration data set. The created model provides a better understanding of the phenomenon and allows other subsidence exposure evaluations to be challenged which will improve an insurance company's management of this risk, given the lack of available subsidence models on the market. This methodology could be improved in the future by using policy level data with a more accurate temporal definition of the claims in order to better apply the created indicators. The framework of this study is also in itself interesting and could be repurposed for other applications. Indeed, the studied models could be extended to other claim prediction problematics, for other types of perils for example, which are often confronted with similar issues of over representation of non-recognized events.

Author contributions. HA provided insurance data and provided technical support. MJ developed the model code and performed the simulations. AC prepared the manuscript with contributions from all co-authors

Competing interests. The authors declare that they have no conflict of interest

Acknowledgements. The authors wish to thank Hélène Gibello, Sonia Guelou, Florence Picard and Franck Vermet for comments on a previous version of the work. Arthur Charpentier received financial support from the Natural Sciences and Engineering Research Council of Canada (NSERC-2019-07077) and the AXA Research Fund.

555

References

R. M. Adelson. Compound poisson distributions. *Journal of the Operational Research Society*, 17(1):73–75, 1966.

V. Antoni, F. Janvier, and C. Albizzati. Retrait-gonflement des argiles: plus de 4 millions de maisons potentiellement très exposées. *Commissariat général au développement durable*, (122), 2017.

Association Française de l'Assurance (AFA). Risques climatiques : quel impact sur l'assurance contre les aléas naturels à l'horizon 2040 ?, 2015.

C. Bergmeir, R. J. Hyndman, and B. Koo. A note on the validity of cross-validation for evaluating autoregressive time series prediction. *Computational Statistics & Data Analysis*, 120:70–83, 2018.

L. Bevere and A. Weigel. Exploring the secondary perils universe. *Swiss Re Sigma*, (1/21), 2021.

P. Bidan and T. Cohignac. Le régime francais des catastrophes naturelles: historique du régime. *Variances*, (11), 2017.

V. Blauhut, K. Stahl, J. H. Stagge, L. M. Tallaksen, L. D. Stefano, and J. Vogt. Estimating drought risk across europe from reported drought impacts, drought indices, and vulnerability factors. *Hydrology and Earth System Sciences*, 20(7):2779–2800, 2016.

R. Bradford. Drought events in europe. In *Drought and drought mitigation in Europe*, pages 7–20. Springer, 2000.

L. Breiman. Bagging predictors. *Machine Learning*, 24(2):123–140, 1996.

L. Breiman. Random forests. *Machine Learning*, (45):5–32, 2001.

L. Breiman, J. H. Friedman, R. A. Olshen, and C. J. Stone. Classification and regression trees. 1983.

A. P. Brignall, M. J. Gawith, J. L. Orr, and P. A. Harrison. Assessing the potential effects of climate change on clay shrinkage-induced land subsidence. In *Climate, Change and Risk*, pages 84–102. Routledge, 2002.

J. Bucheli, T. Dalhaus, and R. Finger. The optimal drought index for designing weather index insurance. *European Review of Agricultural Economics*, 48(3):573–597, 2021.

Caisse Centrale de Réassurance (CCR). Les catastrophe naturelles en france : Bilan 1982 -2019, 2019.

Caisse Centrale de Réassurance (CCR). Arrêtés de catastrophes naturelles, 2020. URL https://catastrophes-naturelles.ccr.fr/les-arretes. Data retrieved from, https://catastrophes-naturelles.ccr.fr/les-arretes.

A. Charpentier. Insurability of climate risks. *The Geneva Papers on Risk and Insurance-Issues and Practice*, 33(1):91–109, 2008.

A. Charpentier, L. Barry, and M. James. Insurance against natural catastrophes: balancing actuarial fairness and social solidarity. *Geneva Papers on Risk & Insurrance*, 2021.

Climate Change Service Climate Data Store (CDS). Copernicus climate change service (c3s) (2017): Era5: Fifth generation of ecmwf atmospheric reanalyses of the global climate., 2020. Data retrieved from Copernicus, https://cds.climate.copernicus.eu/cdsapp#!/home.

T. Corti, V. Muccione, P. Köllner-Heck, D. Bresch, and S. I. Seneviratne. Simulating past droughts and associated building damages in france. *Hydrology and Earth System Sciences*, 13(9):1739–1747, 2009.

T. Corti, M. Wüest, D. Bresch, and S. I. Seneviratne. Drought-induced building damages from simulations at regional scale. *Natural Hazards and Earth System Sciences*, 11(12):3335–3342, 2011.

J. C. Doornkamp. Clay shrinkage induced subsidence. *The Geographical Journal*, 159(2):196–202, 1993.

Entidad Estatal de Seguros Agrarios (ENESA). La sequía, un riesgo incluido en los seguros agrarios. *Noticias Del Seguro*, (82):3–5, 2012.

European Soil Data Centre (ESDAC). Topsoil physical properties for europe (based on lucas topsoil data), 2015. URL esdac.jrc.ec.europa.eu. Data retrieved from Georisque, esdac.jrc.ec.europa.eu.

A. Farahmand and A. AghaKouchak. A generalized framework for deriving nonparametric standardized drought indicators. *Advances in Water Resources*, 76:140–145, 2015.

J. Frécon and F. Keller. Sécheresse de 2003 : un passé qui ne passe pas. rapport d'information fait au nom du groupe de travail sur la situation des sinistrés de la sécheresse de 2003 et le régime d'indemnisation des catastrophes naturelles constitué par la commission des finances. *French Senate Technical Report*, (39), 2009.

Georisques. Gestion assistée des procédures administratives relatives aux risques, 2020. Data retrieved from Georisques, http://www.georisques.gouv.fr/dossiers/telechargement/gaspar.

S. Gourdier and E. Plat. Impact of climate change on claims due to the shrinkage and swelling of clay soils. *Journées Nationales de Géotechnique et de Géologie de l'Ingénieur*, 2018.

N. B. Guttman. Comparing the palmer drought index and the standardized precipitation index. *Journal of the American Water Resources Association*, 34(1):113–121, 1998.

M. Hagenlocher, I. Meza, C. C. Anderson, A. Min, F. G. Renaud, Y. Walz, S. Siebert, and Z. Sebesvari. Drought vulnerability and risk assessments: state of the art, persistent gaps, and research agenda. *Environmental Research Letters*, 14(8):083002, jul 2019.

Z. Hao and A. AghaKouchak. A nonparametric multivariate multi-index drought monitoring framework. *Journal of Hydrometeorology*, 15 (1):89–101, 2014.

G. Herrera-García, P. Ezquerro, R. Tomás, M. Béjar-Pizarro, J. López-Vinielles, M. Rossi, R. M. Mateos, D. Carreón-Freyre, J. Lambert, P. Teatini, et al. Mapping the global threat of land subsidence. *Science*, 371(6524):34–36, 2021.

A. Iglesias, D. Assimacopoulos, and H. van Lanen, editors. *Drought: Science And Policy*. Wiley-Blackwell, Aug. 2019.

M. Ionita and V. Nagavciuc. Changes in drought features at the european level over the last 120 years. *Natural Hazards and Earth System Sciences*, 21(5):1685–1701, 2021.

B. Jørgensen. *The Theory of Dispersion Models*. Chapman & Hall, 1997.

S. Kchouk, L. A. Melsen, D. W. Walker, and P. R. van Oel. A review of drought indices: predominance of drivers over impacts and the importance of local context. *Natural Hazards and Earth System Sciences Discussions*, 2021:1–28, 2021.

M. N. Khaliq, T. B. M. J. Ouarda, P. Gachon, and L. Sushama. Stochastic modeling of hot weather spells and their characteristics. *Climate Research*, 47(3):187–199, 2011.

S. Kok and A. Costa. Framework for economic cost assessment of land subsidence. *Natural Hazards*, 106(3):1931–1949, 2021.

D. Lambert. Zero-inflated poisson regression, with an application to defects in manufacturing. *Technometrics*, 34(1):1–14, 1992.

B. Lloyd-Hughes and M. A. Saunders. A drought climatology for europe. *International Journal of Climatology*, 22(13):1571–1592, 2002.

S. Magnan. Catastrophe insurance system in france. *Geneva Papers on Risk and Insurance. Issues and Practice*, pages 474–480, 1995.

K. A. McCullough. Managing subsidence. *Journal of Insurance Issues*, 27(1):1–21, 2004.

T. B. McKee, N. J. Doesken, and J. Kleist. The relationship of drought frequency and duration to time scales. *Eighth Conference on Applied Climatology*, 1993.

E. Mills. Synergisms between climate change mitigation and adaptation: an insurance perspective. *Mitigation and Adaptation Strategies for Global Change*, 12(5):809–842, 2007.

Ministère de la transition écologique et solidaire (MTES). *Le retrait-gonflement des argiles: Comment prévenir les désordres dans l'habitat individuel*, 2016.

Ministère de l'intérieur (MI). Procédure de reconnaissance de l'état de catastrophe naturelle - révision des critères permettant de caractériser l'intensité des épisodes de sécheresses-réhydrations des sols a l'origine des mouvement de terrains différentiels. Technical report, 2019.

630 Mission des Risques Naturels (MRN). Lettre d'information de la mission des risques naturels, 07 2019.

Mission des Risques Naturels (MRN). Bilan des principaux évènements cat-clim. *Lettre d'information*, (35), 2021.

G. Naumann, J. Spinoni, J. V. Vogt, and P. Barbosa. Assessment of drought damages and their uncertainties in europe. *Environmental Research Letters*, 10(12):124013, dec 2015.

G. Naumann, C. Cammalleri, L. Mentaschi, and L. Feyen. Increased economic drought impacts in europe with anthropogenic warming.
635 *Nature Climate Change*, 11(6):485–491, 2021.

C. D. Pérez-Blanco, G. Delacámara, C. M. Gómez, and S. Eslamian. Crop insurance in drought conditions. In *Handbook of Drought and Water Scarcity, volume 1*, pages 423–444. CRC Press, 2017.

J. Pohjankukka, T. Pahikkala, P. Nevalainen, and J. Heikkonen. Estimating the prediction performance of spatial models via spatial k-fold cross validation. *International Journal of Geographical Information Science*, 31(10):2001–2019, 2017.

640 K. Revfeim. An initial model of the relationship between rainfall events and daily rainfalls. *Journal of Hydrology*, 75(1):357–364, 1984.

R. Schwarze, M. Schwindt, H. Weck-Hannemann, P. Raschky, F. Zahn, and G. G. Wagner. Natural hazard insurance in europe: tailored responses to climate change are needed. *Environmental Policy and Governance*, 21(1):14–30, 2011.

J.-M. Soubeyroux, J.-P. Vidal, J. Najac, N. Kitova, M. Blanchard, P. Dandin, E. Martin, C. Pagé, and F. Habets. Projet climsec : Impact du changement climatique en france sur la sécheresse et l'eau du sol. *Hal-archive*, (00778604), 2011.

645 J.-M. Soubeyroux, N. Kitova, M. Blanchard, J.-P. Vidal, E. Martin, and P. Dandin. Caractérisation des sècheresses des sols en France et changement climatique : Résultats et applications du projet ClimSec. *La Météorologie*, 78:p. 21 – p. 30, 2012.

T. Soyka. A crack in the wall of your home: it could be subsidence, an almost invisible natural hazard. *Swiss Re*, 2021.

J. Spinoni, G. Naumann, H. Carrao, P. Barbosa, and J. Vogt. World drought frequency, duration, and severity for 1951–2010. *International Journal of Climatology*, 34(8):2792–2804, 2014.

650 J. Spinoni, G. Naumann, J. Vogt, and P. Barbosa. European drought climatologies and trends based on a multi-indicator approach. *Global and Planetary Change*, 127:50–57, 2015.

J. Spinoni, G. Naumann, and J. V. Vogt. Pan-european seasonal trends and recent changes of drought frequency and severity. *Global and Planetary Change*, 148:113–130, 2017.

C. Svensson, J. Hannaford, and I. Prosdocimi. Statistical distributions for monthly aggregations of precipitation and streamflow in drought
655 indicator applications. *Water Resources Research*, 53(2):999–1018, 2017.

M. Svoboda and B. Fuchs. *Handbook of Drought Indicators and Indices*. World Meteorological Organization, 2016.

H. Torelló-Sentelles and C. Franzke. Drought impact links to meteorological drought indicators and predictability in spain. *Hydrology and Earth System Sciences Discussions*, 2021:1–32, 2021.

D. Tsegai and I. Kaushik. Drought risk insurance and sustainable land management: what are the options for integration? In *Current*
660 *Directions in Water Scarcity Research*, volume 2, pages 195–210. Elsevier, 2019.

W. Vroege, T. Dalhaus, and R. Finger. Index insurances for grasslands–a review for europe and north-america. *Agricultural systems*, 168: 101–111, 2019.

M. Wües, D. Bresch, and T. Corti. The hidden risks of climate change: An increase in property damage from soil subsidence in europe. *Swiss Re*, (06/11), 2011.